AD-A129 462 CALCULATION OF BOUNDARY LAYERS NEAR THE STAGNATION POINT OF AN OSCILLATIN..(U) NATIONAL AERONAUTICS AND SPACE ADMINISTRATION MOFFETT FIELD C.. T CEBECI ET AL. 1/1

UNCLASSIFIED MAY 83 NASA-A-9143 USAAVRADCOM-TR-83-A-1 F/G 20/4 NL

END
DATE FILMED
7 83
DTIC

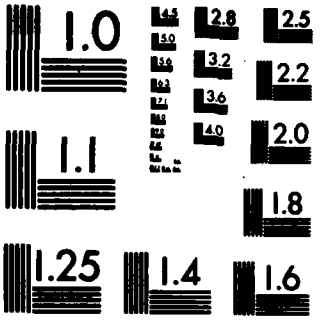

NASA Technical Memorandum 84305

USAAVRADCOM Technical Report 83-A-1

(12)

Calculation of Boundary Layers Near the Stagnation Point of an Oscillating Airfoil

Tuncer Cebeci and Lawrence W. Carr

May 1983

National Aeronautics and Space Administration

United States Army Aviation Research and Development Command

NASA Technical Memorandum 84305

USAAVRADCOM Technical Report 83-A-1

Calculation of Boundary Layers Near the Stagnation Point of an Oscillating Airfoil

Tuncer Cebeci, Mechanical Engineering Department, California State University, Long Beach, CA

Lawrence W. Carr, Aeromechanics Laboratory, AVRADCOM Research and Technology Laboratories, Ames Research Center, Moffett Field, CA

National Aeronautics and Space Administration

Ames Research Center
Moffett Field, California 94035

United States Army
Aviation Research and Development Command
St. Louis, Missouri 63166

CALCULATION OF BOUNDARY LAYERS NEAR THE STAGNATION POINT OF AN OSCILLATING AIRFOIL

Tuncer Cebeci* and Lawrence W. Carr

Ames Research Center
and
Aeromechanics Laboratory
AVRADCOM Research and Technology Laboratories

SUMMARY

The results of an investigation of boundary layers close to the stagnation point of an oscillating airfoil are reported. Two procedures for generating initial conditions — the characteristic-box scheme and a quasi-static approach — were investigated, and the quasi-static approach was shown to be appropriate provided the initial region was far from any flow separation. With initial conditions generated in this way, the unsteady boundary-layer equations were solved for the flow in the leading-edge region of a NACA 0012 airfoil oscillating from 0° to 5°. Results were obtained for both laminar and turbulent flow, and, in the latter case, the effect of transition was assessed by specifying its occurrence at different locations. The results demonstrate the validity of the numerical scheme and suggest that the procedures should be applied to the calculation of the entire flow around oscillating airfoils.

INTRODUCTION

The calculation of boundary-layer characteristics of an oscillating airfoil differs from the usual unsteady flow calculations in that difficulties are caused by the translation of the stagnation point in space and time. In particular, it is essential to develop a procedure to generate initial conditions in the immediate vicinity of the moving stagnation point and to account for the flow reversal that occurs in this region.

The study reported here is the continuation of the work described in reference 1. It is one phase of a study that will be extended later to compute the complete boundary layer and inviscid flow characteristics of an oscillating airfoil in order to improve understanding of the dynamic-stall problem. In the present study, we focus our attention on the calculation of boundary layers near the stagnation point of an oscillating airfoil. We consider both laminar and turbulent flows and two different procedures for generating the initial conditions in the (t,y) plane.

The following section describes the basic equations, turbulence model, the initial conditions and the solution method. The details of the numerical procedure were discussed in reference 1 and are not repeated here.

---

*Mechanical Engineering Dept., California State University, Long Beach, California 90840.

The third section presents the results for NACA 0012 airfoil. Calculations were first performed with two procedures to investigate the prediction of initial conditions in the (t,y) plane. They were limited to laminar flow and to the neighborhood of the leading edge of the airfoil. The next set of calculations involved the boundary-layer behavior of the NACA 0012 airfoil oscillating between angles of attack of 0° and 5° for laminar, transitional, and turbulent flows and for a chord Reynolds number of 3×10^6. The transition location was varied in order to investigate its influence on flow separation.

BASIC EQUATIONS

Boundary-Layer Equations

The boundary-layer equations for an incompressible laminar or turbulent flow on an oscillating airfoil are well known and, with the eddy-viscosity (ε_m) concept, can be written as

$$\frac{\partial u}{\partial x} + \frac{\partial v}{\partial y} = 0 \tag{1}$$

$$\frac{\partial u}{\partial t} + u\frac{\partial u}{\partial x} + v\frac{\partial u}{\partial y} = \frac{\partial u_e}{\partial t} + u_e\frac{\partial u_e}{\partial x} + \frac{\partial}{\partial y}\left(b\frac{\partial u}{\partial y}\right) \tag{2}$$

where x denotes distance along the surface of the airfoil, y is distance along the normal, and $b = \nu + \varepsilon_m$. In the absence of mass transfer, equations (1) and (2) are subject to boundary conditions given by

$$y = 0\ ; \quad u = v = 0\ ; \quad y = \delta\ ; \quad u = u_e(x,t) \tag{3}$$

The presence of the eddy viscosity ε_m requires a turbulence model; we use the algebraic eddy-viscosity formulation developed by Cebeci and Smith (ref. 2). According to this formulation, ε_m is defined by two separate formulas. In the inner region of the boundary layer $(\varepsilon_m)_i$ is defined as

$$(\varepsilon_m)_i = \{0.4y[1 - \exp(-y/A)]\}^2\left|\frac{\partial u}{\partial y}\right|\gamma_{tr} \qquad 0 \le y \le y_c \tag{4}$$

where

$$A = 26\nu u_\tau^{-1}[1 - 11.8\,p^+]^{-1/2}\ , \quad u_\tau = \left(\frac{\tau}{\rho}\right)_{max}^{1/2}\ , \quad p^+ = \frac{\nu u_e}{u_\tau^3}\frac{\partial u_e}{\partial x} \tag{5}$$

In equation (4), γ_{tr} is an intermittency factor that accounts for the transitional region that exists between a laminar and turbulent flow. It is defined by

$$\gamma_{tr} = 1 - \exp\left[-G(x - x_{tr})\int_{x_{tr}}^{x}\frac{dx}{u_e}\right] \tag{6}$$

Here x_{tr} is the location of the start of transition and the empirical factor G, which has the dimensions of velocity/(length)^2, is given by (ref. 2)

$$G = \frac{1}{1200} \frac{u_e^3}{\nu^2} R_{x_{tr}}^{-1.34} \tag{7}$$

The transition Reynolds number is defined as $R_{x_{tr}} = (u_e x/\nu)_{tr}$.

In the outer region, $(\varepsilon_m)_o$ is defined as

$$(\varepsilon_m)_o = 0.0168 \left| \int_0^\infty (u_e - u)dy \right| \gamma_{tr} \qquad y_c \le y \le \infty \tag{8}$$

The boundary between the inner and outer regions, y_c, is established by the continuity of the eddy-viscosity formulas.

Initial Conditions

If initial conditions in the (t,y) plane are given at a station x_o on the upper surface of the airfoil and satisfy the condition $u > 0$ and, in addition, initial conditions are given in the (x,y) plane at $t = 0$, then the solutions of equations (1), (2), and (3) may be integrated in $x > x_o$ until they break down (flow separation). A similar remark applies to the lower surface except that $u < 0$. The initial conditions at $t = 0$ can be generated for both surfaces if steady conditions are assumed to prevail at that time. It is only necessary to solve the appropriate equations which, in this case, are given by equation (1) and by

$$u \frac{\partial u}{\partial x} + v \frac{\partial u}{\partial y} = u_e \frac{du_e}{dx} \frac{\partial}{\partial y} \left(b \frac{\partial u}{\partial y} \right) \tag{9}$$

There is no problem with the initial conditions for equations (1) and (9) since the calculations start at the stagnation point $x = x_s$, where u_e and u are zero for all y.

Unlike steady flows, where u_e and u are zero for all y at the stagnation point, the stagnation point is not fixed in an unsteady flow; although u_e is zero, we cannot assume a priori that u is also zero. We may avoid these difficulties by using an implicit method, but now we are faced with the problem of generating a starting profile on the new time-line.

A convenient and accurate procedure for calculating the first velocity profile at the new time-line has been developed (ref. 1); it involves the use of the "characteristic-box" scheme developed by Cebeci and Stewartson (in ref. 3) and described in ref. 1. Another procedure, though not as accurate, is to use a quasi-steady approach in the immediate vicinity of the stagnation point region. We shall discuss both procedures later (Results and Discussion section).

Transformed Equations

As in previous studies (see, for example, ref. 4), we use similarity variables to transform the governing equations before we seek their solution. For a steady flow, we use the Falkner-Skan transformation defined by

$$\eta = \frac{(u_e)^{1/2} y}{\nu x} , \quad \psi = (u_e \nu x)^{1/2} f(x,\eta) \tag{10}$$

where ψ is the usual definition of stream function that satisfies the continuity equation (1), that is

$$u = \frac{\partial \psi}{\partial y} , \quad v = - \frac{\partial \psi}{\partial x} \tag{11}$$

With this transformation, equation (9) and its boundary conditions, equation (3), can be written as

$$(bf'')' + \frac{m+1}{2} ff'' + m[1 - (f')^2] = x\left(f' \frac{\partial f'}{\partial x} - f'' \frac{\partial f}{\partial x}\right) \tag{12}$$

$$\eta = 0 ; \quad f = f' = 0 ; \quad \eta = \eta_e ; \quad f' = 1 \tag{13}$$

where primes denote differentiation with respect to η, and m denotes a dimensionless pressure-gradient parameter defined by

$$m = \frac{x}{u_e} \frac{du_e}{dx} \tag{14}$$

For unsteady flows, we use a transformation similar to that defined by equation (10) except that u_e is now a function of both x and t, and the dimensionless stream function F is a function of x, t, and ζ; we let

$$\zeta = \frac{[u_e(x,t)]^{1/2}}{\nu x} y , \quad \psi = [u_e(x,t)\nu x]^{1/2} F(x,t,\zeta) \tag{15}$$

With this transformation, it can be shown that the continuity and momentum equations and their boundary conditions for unsteady incompressible flows can be written as

$$(bF'')' + \frac{m+1}{2} FF'' + m[1 - (F')^2] + m_s(1 - F') - \frac{\zeta}{2} m_s F'' = x \frac{1}{u_e} \frac{\partial F'}{\partial t} + F' \frac{\partial F'}{\partial x} - F'' \frac{\partial F}{\partial x} \tag{16}$$

$$\zeta = 0 ; \quad F = F' = 0 ; \quad \zeta = \zeta_e ; \quad F' = 1 \tag{17}$$

Here primes now denote differentiation with respect to ζ and

$$m = \frac{x}{u_e} \frac{\partial u_e}{\partial x} , \quad m_s = \frac{x}{u_e^2} \frac{\partial u_e}{\partial t} , \quad b = 1 + \epsilon_m^+ , \quad \epsilon_m^+ = \frac{\epsilon_m}{\nu} \tag{18}$$

Solution Procedure

We use Keller's box method to solve the governing equations of the previous section. This is a two-point finite-difference method which has been used to solve a

wide range of parabolic partial-differential equations, as discussed in reference 4. The solution procedure for equations (12) and (13) is identical to that described in reference 5. The solution procedure employing the characteristic box scheme to generate the first velocity profile at a new time-line is described in reference 1. For unsteady flows, where we now solve equations (16) and (17), we use the solution procedure described in reference 6. In regions where there are no flow reversals across the layer, we use the "standard box" scheme and in regions where there is flow reversal, we use the "zig-zag" scheme.

A Model for External Velocity Distribution

The solution of boundary-layer equations requires that the external velocity distribution be specified. Since the present effort is directed toward solutions near the leading edge of the airfoil, a local model for the potential flow has been chosen in the place of a full-potential flow code. We first consider an ellipse with major axis $2a$ and thickness ratio T, where $2aX$ and $2AY$, respectively, measure distance along and perpendicular to the major axis from one apse, that is, from the nose. The equation of the ellipse is then

$$4\left(X - \frac{1}{2}\right)^2 + \frac{4Y^2}{T^2} = 1 \tag{19}$$

and the velocity distribution near the nose is given by (ref. 6)

$$\frac{u_e}{u_\infty} = \pm \frac{(1 + T)(X^{1/2} \pm \alpha)}{[X + (1/4)T^2]^{1/2}} \tag{20}$$

where α is proportional to the angle of attack in radians. Here T denotes the thickness ratio ($\equiv b/a$) and (+) denotes the upper surface and (-) the lower surface. We note that equation (20) is valid only when $\alpha = 0(T)$, $X = 0(T^2)$, and the location of the stagnation point X_s is $X_s = \alpha^2$.

The external velocity distribution of a symmetrical airfoil in the neighborhood of the nose can also be represented by an expression similar to equation (20). It is only necessary to let T denote the thickness ratio of the equivalent ellipse and replace $T^2/4$ by $R/2$, where R is the nose radius. For example, the nose region of a NACA 0012 airfoil at an angle of attack of 5° can be represented by the ellipse by matching three points (0, 0.2, and 0.12); then the appropriate form of equation (20) is

$$\frac{u_e}{u_\infty} = \pm 1.2065 \frac{(X^{1/2} \pm 4.783)}{(X + 0.00613)^{1/2}} \tag{21}$$

Figure 1 shows a comparison of the external velocity distribution computed by the inviscid flow theory and that computed by equation (21) for the lower and upper surfaces of a NACA 0012 airfoil. Equation (21) is thus a satisfactory fit for the velocity distribution extending to approximately 20% chord.

Equation (21) can also be used to approximate the external velocity distribution, when the angle of attack is varying sinusoidally, by writing it as

$$\frac{u_e}{u_\infty} = \pm 1.2065 \frac{[X^{1/2} \pm 0.957\alpha(1 + A \sin \omega t)]}{(X + 0.00613)^{1/2}} \tag{22}$$

Here physical time is $u_\infty t/c$, the period of oscillation of the airfoil is $2\pi c/u_\infty w$, c (= 2a) is the chord, and A is a free parameter. We note from equation (8) that at time t = 0, the external velocity distribution corresponds to that given by steady state. By choosing A = 1 and $\alpha = 5°$, we can compute the velocity distribution at angles of attack ranging from 0° to 10°. The term

$$0.957\alpha(1 + A \sin \omega t) \tag{23}$$

can be interpreted as an effective angle of attack, $\alpha_{eff}(t)$. With this definition, equation (23) becomes

$$\frac{u_e}{u_\infty} = \pm 1.2065 \frac{[X^{1/2} \pm \alpha_{eff}(t)]}{(X + 0.00613)^{1/2}} \tag{24}$$

Figure 2 shows a comparison of the external velocity distribution computed by Neumann and by equation (24) for $\alpha = 0°$ and 10°. As can be seen, equation (24) is a satisfactory representation of the velocity distribution, especially near the leading edge. We note from the results that the agreement begins to deteriorate on the upper surface as α_{eff} begins to increase. However, equation (24) is a convenient formula for generating the external velocity distribution in the immediate vicinity of the stagnation point and for testing the computer program.

RESULTS AND DISCUSSION

Calculation of Initial Conditions by Two Separate Procedures

The procedure, based on the so-called characteristic-box scheme and developed for calculating the initial conditions in the (t,y) plane, was tested for a model problem (ref. 1) in which the external velocity distribution was given by

$$u_e = \frac{\xi + \xi_o(1 + A \sin \omega t)}{(1 + \xi)^2]^{1/2}} \tag{25}$$

Here $X = (1/4)T^2\xi^2$, $\xi = O(1)$, and A and ξ_o denote parameters that need to be specified. The latter can be regarded as a reduced angle of attack; if it is increased beyond 1.155, the steady-state solution at t = 0 separates on the upper surface of the airfoil. Calculations were carried out with this procedure (ref. 1) for a test case — $\xi_o = 0.10$, A = 1, $\omega = \pi/4$ — for a limited range of $x(|x| < 0.3)$, and the formal validity and efficacy of the numerical scheme was established.

When this procedure was used for the external velocity distribution given by equation (24) with $\omega = 0.1$, a value typical of conditions of dynamic stall, the computing time of the numerical procedure increased significantly and the unsteady effects on the stagnation-point behavior decreased. For this reason, an alternative procedure based on a quasi-steady approach was developed and its results were compared with the predictions of the procedure of reference 1. With the quasi-steady approach, the stagnation point was computed from equation (24) and the solution of

the boundary-layer equations was obtained up to $X = 0.005$ ($= X_o/c$). Because of the rapid variation of the external velocity distribution in the stagnation-point region, extremely small values in Δx corresponding to 0.001 were taken. Since the quasi-steady approach is not valid for flows approaching separation, x_o/c was chosen to be just upstream of the pressure minimum and the calculations were then limited to the region where the pressure gradient was favorable.

Figure 3 shows a comparison of the predictions of both procedures. The calculations were performed with initial conditions in the (x,y) plane corresponding to a steady flow with an effective angle of attack α of 5° and for the external velocity distribution given by equation (24). The parameter A was set equal to 1 and the reduced frequency was equal to 0.1. The largest effective angle of attack was 10°, corresponding to $\omega t = \pi/2$, and the calculations were limited to the quarter cycle from zero to $\pi/2$. It is expected that any differences between the results of the two procedures would be greatest in this range, especially close to $\pi/2$.

The results shown in figure 3 indicate that the computed values of local skin-friction coefficient obtained by both procedures are in remarkable agreement with each other. (The small difference in c_f stems from the use of different Δx-spacings.) The procedure that uses the characteristic-box approach requires much smaller Δx-spacings than the quasi-steady approach, without offering significant improvement in prediction accuracy. The quasi-steady approach is easier to use (than the characteristic-box approach), less demanding of computer time, and of equivalent accuracy in the region of the stagnation point; as a result, we found it convenient for use in the present study. This conclusion is, however, limited to the generation of initial conditions near the stagnation point and to situations far from separation.

It is of interest to investigate the reason for the success of the quasi-steady approximation in this study in contrast to the earlier one (ref. 1), in which the behavior of the stagnation line is too complicated to be satisfactorily approximated in this way. Examination of equation (24) shows that the range of values of X over which u_e varies by a significant amount is quite small; for $\alpha_{eff} = 5°$, u_e increases from zero at $X^{1/2} = -0.084$ to a maximum of $1.77u_\infty$ at $X = 0.005$, the corresponding values of x/c being -0.082 and $+0.073$. Thus, in equation (2), $u(\partial u/\partial x) \sim 20u_\infty^2/c$, and $\partial u/\partial t \sim (\omega u_\infty/c)u_\infty = 0.1u_\infty^2/c$. Hence, in retrospect it is not surprising that the unsteady term in equation (1) may be neglected in comparison with the steady inviscid terms when computing the boundary-layer structure near the forward stagnation point. Further downstream, $u(\partial u/\partial x)$ becomes much smaller and the neglect of $\partial u/\partial t$ is not necessarily justifiable. Indeed, if separation occurs, it is crucial that the $\partial u/\partial t$ term be retained in the integration; otherwise, the solution will develop a singularity when the skin-friction vanishes.

The results of the present study may be generalized into the working rule that if the frequency of oscillation is $\omega^*/2\pi$, if R is the nose radius of the airfoil, and if $\omega^* R/u_\infty < 0.1$, then the quasi-steady approximation may be used to compute the boundary layer near the nose on the compression side, and as far as the pressure minimum on the suction side. For the calculation reported in reference 1, the value of ω in equation (25) was taken to be $\pi/4$. Thus the two inertial terms, $\partial u/\partial t$ and $u(\partial u/\partial x)$, in equation (1) are approximately of the same order of magnitude near the forward stagnation point and neither could safely be neglected.

Boundary-Layer Behavior of a NACA 0012 Airfoil Near the Leading Edge

With the initial conditions computed by the quasi-steady approach, calculations were performed to investigate the boundary-layer behavior of the NACA 0012 airfoil near its leading edge at different angles of attack for a reduced frequency of 0.1 and for a chord Reynolds number of 3×10^6. Calculations were first performed for angles of attack in the range of 0° to 5°. The expression for the effective angle given by equation (23) was written as

$$\alpha_{eff} = \frac{0.957\alpha}{2}(1 - \cos \omega t) \tag{26}$$

so that the steady-state calculations start for zero angle of attack and, for half a cycle, unsteady flow calculations were performed as the angle of attack was varied from 0° to 5° by taking $\alpha = 5°$ in equation (26). Results were obtained for both laminar and turbulent flows, with the transition point specified at $(X/c)_{tr} = 0.06$.

Figure 4 shows the variation of wall-shear parameter F''_w and displacement thickness δ^*, defined by

$$\delta^* = \int_0^\infty \left(1 - \frac{u}{u_e}\right) dy \tag{27}$$

with X for three effective angles: $\alpha_{eff} = 0$, 2.5, and 5. We see that the location of minimum wall shear occurs at the transition point, namely $(X/c)_{tr} = 0.06$, which moves upstream with increasing angle of attack, for example, to $X/c = 0.05$ at $\alpha_{eff} = 5°$. The displacement thickness reaches a maximum, for example, at $X/c = 0.06$ for $\alpha_{eff} = 0°$, reduces to a minimum after transition, and increases again with further increase in X. The effect of angle of attack on displacement thickness is pronounced, and at $\alpha_{eff} = 5°$, the displacement thickness reaches a maximum of $X/c = 0.06$, with a large dip in the $\Delta X/c$ range of 0.03, before it increases again.

Calculations were next performed for the same angle-of-attack range, but this time the effective angle given by equation (23) was written as

$$\alpha_{eff} = \frac{0.957\alpha}{2}(1 + \sin \omega t) \tag{28}$$

so that the steady-state calculations started at an angle of attack of 2.5°. Unsteady calculations were performed for one cycle by taking 10° increments in time. The transition point was specified at two different X-locations to determine its effect.

Figures 5 and 6 show the variation of wall-shear parameter F''_w and displacement thickness δ^* with X for the same effective angles as those in figure 4, but with $(X/c)_{tr} = 0.04$ and 0.07, respectively. The minimum value of wall shear in figure 5 occurs at the transition point, namely $(X/c)_{tr} = 0.04$ for steady-state conditions with $\alpha_{eff} = 2.5°$ and moves downstream with decreasing angle of attack; for example, to $X/c = 0.044$ at $\alpha_{eff} = 0°$ and upstream with increasing angle of attack to $X/c = 0.036$ at $\alpha_{eff} = 5°$. As in figure 4, the effect of angle of attack on displacement thickness is pronounced as α_{eff} increases from 0° to 5° causing a large dip in δ^*.

The results of figure 6 were obtained for a delayed transition location of $(X/c)_{tr} = 0.07$ and show similar behavior of wall shear and displacement thickness with X at different angles of attack. Since the region of laminar flow has increased, the values of wall shear are lower, indicating that the flow may approach separation conditions with further delay of transition. The minimum value of wall shear again occurs at the transition point, $(X/c)_{tr} = 0.07$, with increasing or decreasing angle of attack as it moves upstream, for example, to $X/c = 0.065$ at $\alpha_{eff} = 0°$ and to $X/c = 0.06$ at $\alpha_{eff} = 5°$.

CONCLUDING REMARKS

A method for calculating the behavior of laminar and turbulent boundary layers on an oscillating airfoil has been developed and used to obtain results for the boundary layer around a NACA 0012 airfoil oscillating between 0° and 5°. Two procedures for generating the initial conditions in the (t,y) plane were investigated — a characteristic box scheme and a quasi-static approach. The quasi-static approach was shown to be preferable provided the X-location was far from flow separation. The boundary-layer results were obtained by solving the unsteady-flow equations for different angles of attack for both laminar and turbulent flows. They allow comparison of laminar and turbulent flow and for the latter, quantify the effect of changing the location of transition. They are presented in terms of displacement thickness and wall-shear parameter, both of which show large differences at the larger angles of attack.

REFERENCES

1. Cebeci, T.; and Carr, L. W.: Prediction of Boundary-Layer Characteristics of an Oscillating Airfoil. Unsteady Turbulent Shear Flows, R. Michel, J. Cousteix, and R. Houdeville, eds., IUTAM Symposium, Toulouse, France, 1981.

2. Cebeci, T.; and Smith, A. M. O.: Analysis of Turbulent Boundary Layers. Academic Press, New York, 1974.

3. Bradshaw, P.; Cebeci, T.; and Whitelaw, J. H.: Engineering Calculation Methods for Turbulent Flows. Academic Press, London, 1981.

4. Cebeci, T.; and Bradshaw, P.: Momentum Transfer in Boundary Layers. McGraw-Hill/ Hemisphere, Washington, D.C., 1977.

5. Cebeci, T.; and Carr, L. W.: Computation of Unsteady Turbulent Boundary Layers with Flow Reversal and Evaluation of Two Separate Turbulence Models. Also NASA TM-81259; USAAVRADCOM TR 81-A-5.

6. Lamb, H.: Hydrodynamics. University Press, Cambridge, 1932.

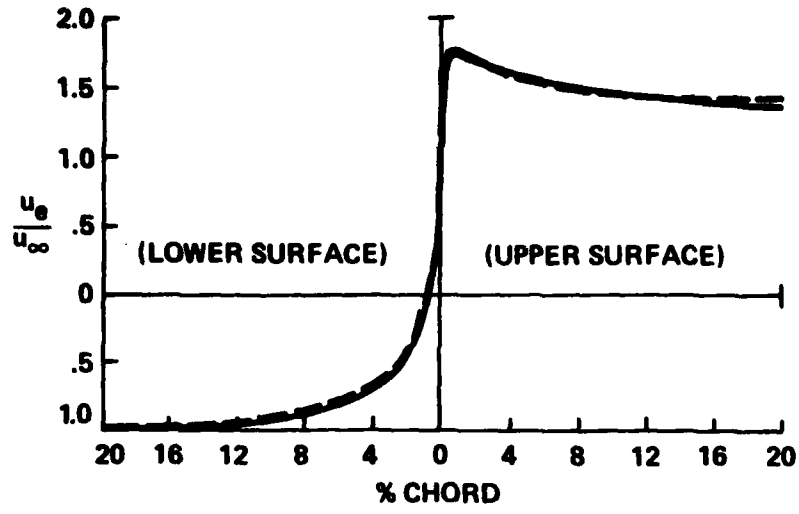

Figure 1.- Comparison of inviscid velocity distribution computed by Neumann (solid line) and those computed by equation (21) (dashed lines) for $\alpha = 5$ (NACA 0012 airfoil).

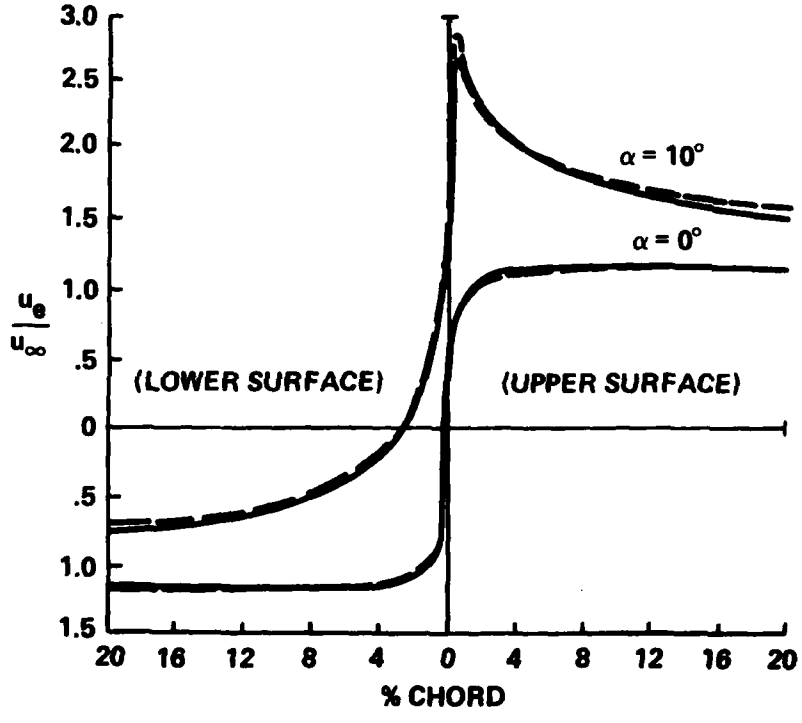

Figure 2.- Comparison of inviscid velocity distribution computed by Neumann (solid lines) and those computed by equation (24) (dashed lines) for $\alpha = 0°, 10°$.

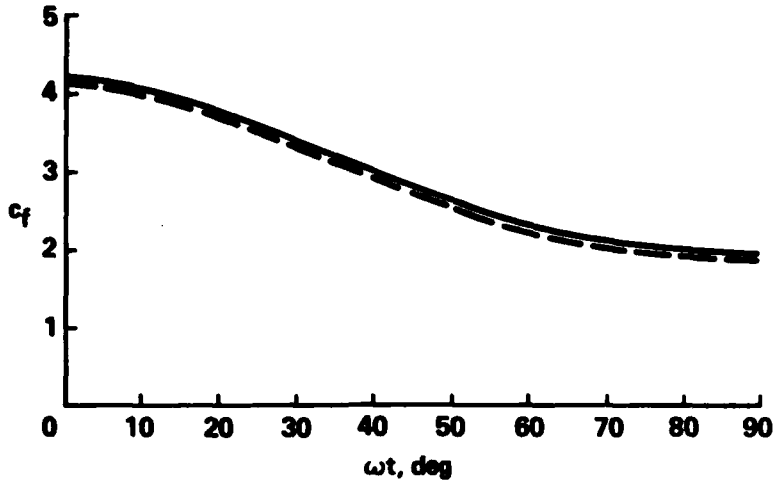

Figure 3.- Comparison of the predictions of two separate procedures for computing initial conditions in the (t,y) plane. Solid lines denote the solutions obtained by the characteristic box scheme described in reference 1; the dashed lines denote those obtained with the quasi-steady approach.

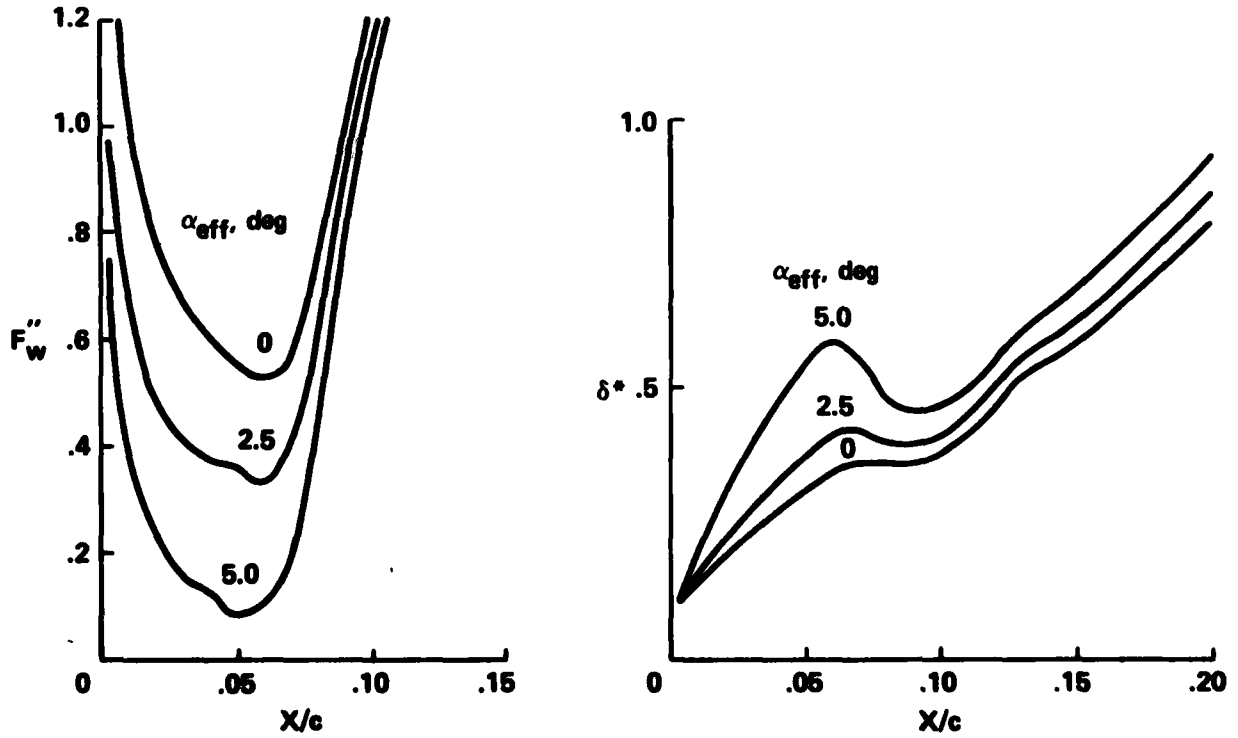

(a) Wall-shear parameter F''_w.

(b) Displacement thickness δ^*.

Figure 4.- Variation of wall-shear parameter and displacement thickness with X/c for NACA 0012 airfoil with transition set at X/c = 0.06; the effective angle of attack is given by equation (26).

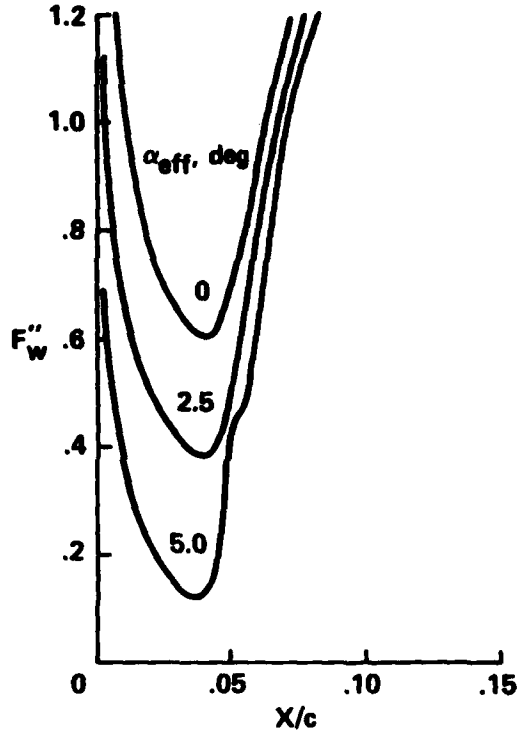

(a) Wall-shear parameter F''_w.

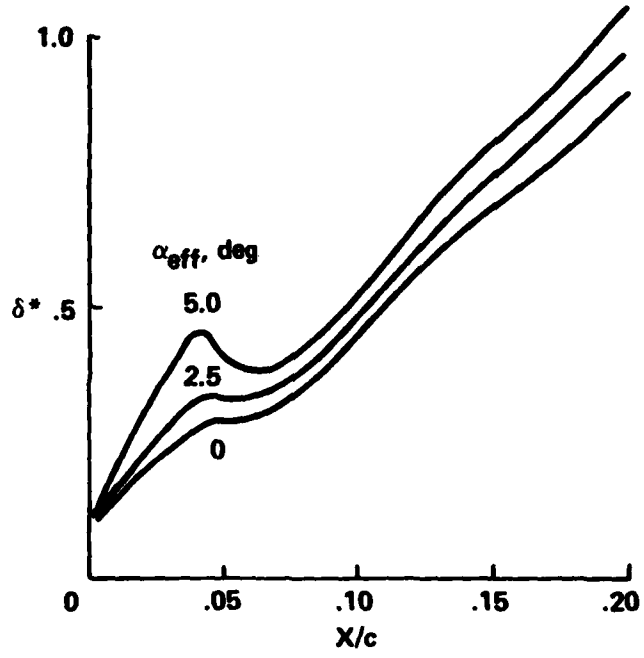

(b) Displacement thickness δ^*.

Figure 5.- Variation of wall-shear parameter and displacement thickness with X/c for NACA 0012 airfoil with transition set at X/c = 0.04; the effective angle of attack is given by equation (28).

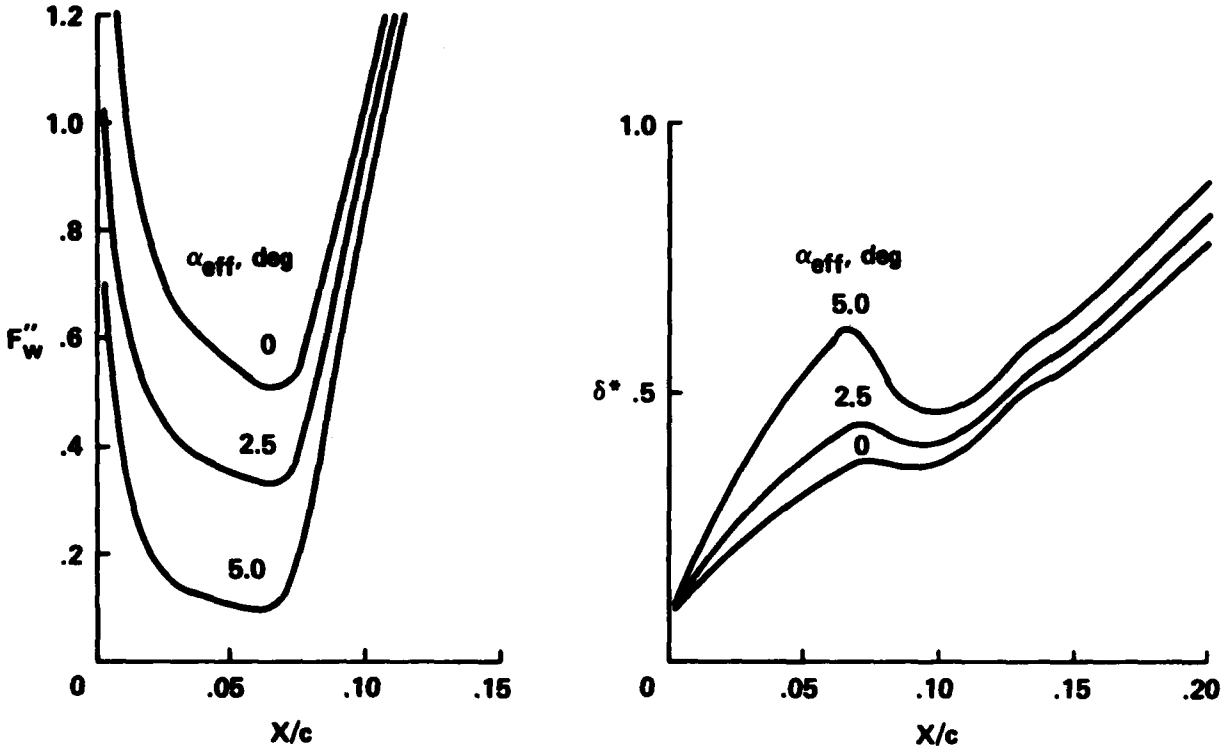

(a) Wall-shear parameter F''_w.

(b) Displacement thickness δ^*.

Figure 6.- Variation of wall-shear parameter and displacement thickness with X/c for NACA 0012 airfoil with transition set at X/c = 0.07; the effective angle of attack is given by equation (28).

1. Report No.	2. Government Accession No.	3. Recipient's Catalog No.
NASA TM	AD-A129462	

4. Title and Subtitle
CALCULATION OF BOUNDARY LAYERS NEAR THE STAGNATION POINT OF AN OSCILLATING AIRFOIL

5. Report Date
May 1983

6. Performing Organization Code

7. Author(s)
Tuncer Cebeci* and Lawrence W. Carr

8. Performing Organization Report No.
A-9143

10. Work Unit No.
K 1585

9. Performing Organization Name and Address
*Mechanical Engineering Dept., Calif. State Univ., Long Beach, CA 90840
NASA Ames Research Center and
AVRADCOM Research and Technology Laboratories
Moffett Field, Calif. 94035

11. Contract or Grant No.

13. Type of Report and Period Covered
Technical Memorandum

12. Sponsoring Agency Name and Address
National Aeronautics and Space Administration, Washington, D.C. 20546 and U.S. Army Aviation Research and Development Command, St. Louis, Mo. 63166

14. Sponsoring Agency Code

15. Supplementary Notes
Point of Contact: L. W. Carr, Aerodynamic Research Branch, Ames Research Center, MS 227-8, Moffett Field, Calif. 94035 (415)965-6265 or FTS 448-6265.

16. Abstract

The results of an investigation of boundary layers close to the stagnation point of an oscillating airfoil are reported. Two procedures for generating initial conditions — the characteristics-box scheme and a quasi-static approach — were investigated, and the quasi-static approach was shown to be appropriate provided the initial region was far from any flow separation. With initial conditions generated in this way, the unsteady boundary-layer equations were solved for the flow in the leading-edge region of a NACA 0012 airfoil oscillating from 0^{deg} to 5^{deg}. Results were obtained for both laminar and turbulent flow, and, in the latter case, the effect of transition was assessed by specifying its occurrence at different locations. The results demonstrate the validity of the numerical scheme and suggest that the procedures should be applied to calculation of the entire flow around oscillating airfoils.

17. Key Words (Suggested by Author(s))	18. Distribution Statement	
Dynamic stall Oscillating airfoils Boundary layers Unsteady boundary layers Unsteady viscous flow	Unlimited Subject Category — 34	

19. Security Classif. (of this report)	20. Security Classif. (of this page)	21. No. of Pages	22. Price*
Unclassified	Unclassified	17	A03

*For sale by the National Technical Information Service, Springfield, Virginia 22161